Available online at www.sciencedirect.com
ScienceDirect
Tetrahedron 64 (2008) 3153–3159
Tetrahedron
www.elsevier.com/locate/tet

A highly enantioselective chiral Schiff-base fluorescent sensor for mandelic acid

Koushik Dhara [a], Krishanu Sarkar [b], Partha Roy [a], Mahasweta Nandi [b], Asim Bhaumik [b], Pradyot Banerjee [a,*]

[a] Department of Inorganic Chemistry, Indian Association for the Cultivation of Science, Jadavpur, Kolkata 700 032, India
[b] Department of Materials Science and Centre for Advanced Materials, Indian Association for the Cultivation of Science, Jadavpur, Kolkata 700 032, India

Received 1 October 2007; received in revised form 3 January 2008; accepted 25 January 2008
Available online 31 January 2008

Abstract

A chiral Schiff-base compound, 4-methyl-2,6-bis-[(2-hydroxy-1-phenylethylimino)methyl]phenol, is found to act as highly enantioselective fluorescent agent for α-hydroxycarboxylic acid, e.g., mandelic acid. It is observed that, within a certain concentration range, one enantiomer of the chiral acid can increase the fluorescence intensity of the Schiff-base compound 122-fold while the other enantiomer enhances the intensity only 42-fold. Such highly enantioselective responses towards the chiral acid make the unusual Schiff-base compound attractive as a fluorescent sensor for determining the enantiomeric composition of α-hydroxycarboxylic acids.
© 2008 Elsevier Ltd. All rights reserved.

Keywords: Chiral Schiff-base; α-Hydroxycarboxylic acid; Enantioselective; Fluorescent sensor

1. Introduction

The luminescent properties of an organic chromophore can be utilized for chiral recognition of a molecule.[1,2] The methodology involved is to introduce a chiral centre by introducing a fluorophore into the binding site so that it can achieve enantioselective recognition of chiral organic molecules. Amines, amino alcohols and hydroxycarboxylic acids have been intensively and widely studied from a viewpoint of their usefulness in synthetic applications.[1] Modern analytical approaches, e.g., high-resolution mass spectroscopy, electronic spectroscopy, electrophoresis etc.[3] are also used for such studies. Although there have been several other methods, e.g., chromatography and NMR techniques, there are significant advantages of using a fluorescent agent.[4–7]

A literature survey shows that the fluorescence properties of the naphthalene moiety in 1,1′-bi-2-naphthol (BINOL) and its derivatives have been previously used as an agent for chiral recognition and asymmetric catalysis.[8–11] Recently we have reported the fluorescence sensing property of a Schiff-base molecule which can bind to zinc(II). X-ray structural analysis and other solution studies showed the formation of a discrete hexanuclear complex on binding where the ratio of zinc/Schiff-base was 3:1.[12] We report here the design and syntheses of Schiff-base molecules (*R*,*R*)-**1** and (*S*,*S*)-**1** (Scheme 1), which can effectively be used as enantioselective fluorescent sensors for mandelic acids. Systematic studies have been performed to get an insight into the intimate mechanisms of such interactions. The choice of mandelic acids as the sensing substrate for detection lies in the fact that it is present in certain skin care products, and is an intermediate molecule in the production of other biochemicals, an analytical reagent and a precursor in the manufacture of certain dyes.[13,14] In the presence of (*S*)- or (*R*)-mandelic acid, (*R*,*R*)-**1** and (*S*,*S*)-**1** exhibit significant fluorescence enhancements owing to suppressed PET (photoinduced-electron-transfer) quenching when the acidic proton of mandelic acid interacts with the nitrogen of the imine nitrogen of the sensor. On complexation, the lone pair of electrons on the nitrogen atom is no longer available for

* Corresponding author. Fax: +91 33 2473 2805.
E-mail address: icpb@mahendra.iacs.res.in (P. Banerjee).

0040-4020/$ - see front matter © 2008 Elsevier Ltd. All rights reserved.
doi:10.1016/j.tet.2008.01.099

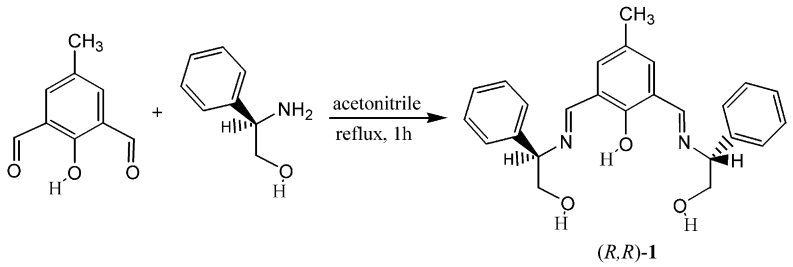

Scheme 1. Synthesis of the chiral Schiff-base (*R*,*R*)-**1** sensor.

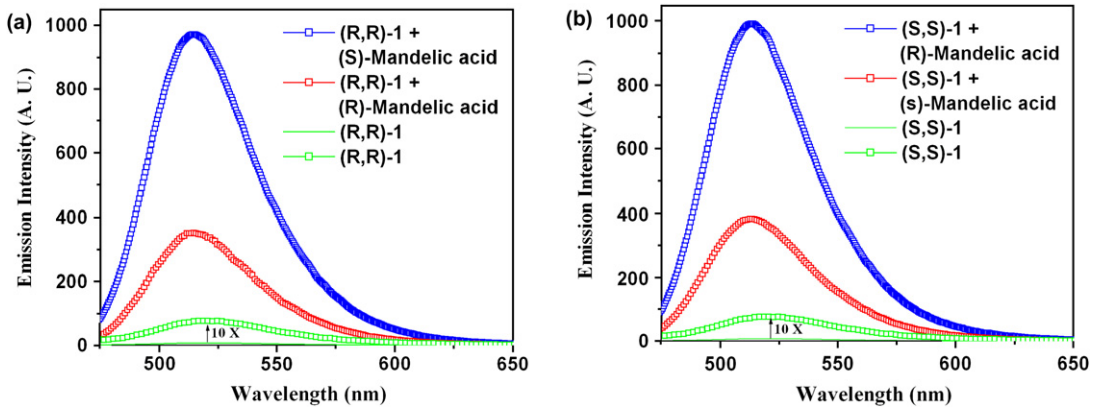

Figure 1. Fluorescence spectra of (a) (*R*,*R*)-**1** and (b) (*S*,*S*)-**1** with and without mandelic acid (λ_{ex}=462 nm).

PET,[15] leading to a fluorescence enhancement. Since the interaction of the sensor with the two enantiomers of mandelic acid should generate two different diastereomers, different fluorescence enhancements can occur.

2. Results and discussion

Compound (*R*,*R*)-**1** was prepared by the Schiff-base condensation between 4-methyl-2,6-diformylphenol and (*R*)-2-amino-2-phenylethanol (Scheme 1) in acetonitrile. Similarly (*S*,*S*)-**1** was synthesized by the same dialdehyde and (*S*)-2-amino-2-phenylethanol. The UV–vis spectrum of (*R*,*R*)-**1** in benzene displays absorption at λ_{max} 277, 353 and 442 nm. It emits at 522 nm on excitation at 462 nm. We have studied the fluorescent recognition of (*R*,*R*)-**1** and (*S*,*S*)-**1** for mandelic acid. A large enhancement was observed when (*R*,*R*)-**1** was treated with (*S*)- or (*R*)-mandelic acid. This behaviour is highly enantioselective. The response of (*R*,*R*)-**1** towards (*S*)- or (*R*)-mandelic acid shows a dramatic difference. As demonstrated in Figure 1a, (*R*)-mandelic acid (3.0×10^{-3} M) has little effect on the fluorescence of (*R*,*R*)-**1** (1.0×10^{-4} M in benzene containing 2% 1,2-dimethoxyethane (DME)). Interestingly, under the same experimental conditions (*S*)-mandelic acid causes a large increase in the fluorescence intensity of (*R*,*R*)-**1**. By way of comparison the increase in the case of (*R*,*R*)-**1** is ca. 122 times with (*S*)-mandelic acid, which falls to ca. 42 times with (*R*)-mandelic acid. We have shown in Figure 2 the change in fluorescence of (*R*,*R*)-**1** and (*S*,*S*)-**1** (1×10^{-4} M in benzene containing 2%

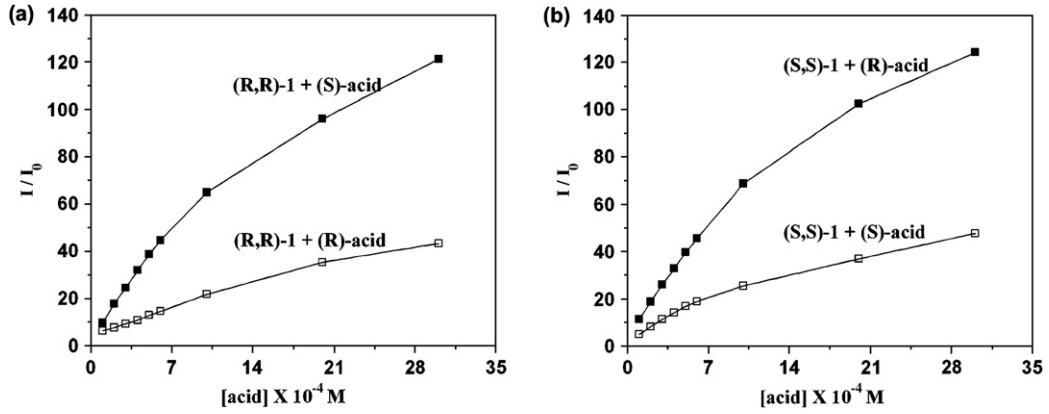

Figure 2. Fluorescence enhancement of (a) (*R*,*R*)-**1** and (b) (*S*,*S*)-**1** (1.0×10^{-4} M in benzene containing 2% DME) versus concentration of (*R*)- and (*S*)-mandelic acid.

DME) in the presence of various concentrations of (*S*)- and (*R*)-mandelic acid. The factor (I_e) related to the fluorescence enhancement of (*R*,*R*)-**1** by (*S*)-mandelic acid may be expressed by $I_e=(I_S-I_0)/(I_R-I_0)$ and assumes a value of 2.9 where I_0, I_S and I_R indicate the emission intensity of (*R*,*R*)-**1** in absence of mandelic acid, in presence of (*S*)-mandelic acid and (*R*)-mandelic acid, respectively. This clearly justifies the suitability of this sensor.[1g]

We studied under identical conditions the fluorescence enhancement of (*S*,*S*)-**1** in the presence of (*R*)- and (*S*)-mandelic acid. The results are displayed in Figure 1b showing the efficiency of (*R*)-mandelic acid over (*S*)-mandelic acid in modulating the fluorescence characteristic of (*S*,*S*)-**1**. As expected, we note a 'reverse image' relationship between the fluorescence enhancement of (*R*,*R*)-**1** and (*S*,*S*)-**1** in the presence of mandelic acid. A 'mirror image' relationship between the fluorescence enhancement of enantiomers (sensors) has been observed earlier.[1]

Time-dependant measurements of (*R*,*R*)-**1** and (*S*,*S*)-**1** in the absence and presence of added mandelic acids have been performed using time-correlated single-photon counting (TCSPC) (Fig. 3). The fluorescence lifetime (τ_f) of (*R*,*R*)-**1** is only 0.90 ns, which is significantly increased to 3.67 and 3.78 ns in the presence of (*R*)- and (*S*)-mandelic acid, respectively. The relative quantum yield (Φ_f) of (*R*,*R*)-**1** increases from 0.12 to 0.58 and 0.66 in the presence of (*R*)- and (*S*)-form of the acid, respectively. According to the equation[16] $\tau^{-1}=k_r+k_{nr}$ and $k_r=\Phi_f/\tau$, the radiative rate constant k_r and total nonradiative rate constant k_{nr} of (*R*,*R*)-**1**, (*S*,*S*)-**1** and the corresponding complexes with acid (2:3 sensor/acid ratio, estimated from Job plot analysis) are calculated and listed in Table 1. The data suggest that k_r has just slightly changed, but the factor that induces fluorescent enhancement is mainly ascribed to the large decrease in k_{nr}. The remarkable difference in τ_f and Φ_f values between (*R*)- and (*S*)-acids is probably due to the generation of two different diastereomeric complexes with the sensor.

Fluorescence titration of a solution of (*R*,*R*)-**1** (1.0×10^{-4} M) with mandelic acid (1.0×10^{-4}–3.0×10^{-3} M) affords data which can be effectively used to extract the association constant (*K*) assuming 1:1 binding, in conjunction with the modified

Table 1
Radiative and total nonradiative rate data of (*R*,*R*)-**1** and (*S*,*S*)-**1** in the presence and absence of mandelic acid

	τ_f (ns)	Φ_f	k_r (10^8 s^{-1})	k_{nr} (10^8 s^{-1})	χ^2
(*R*,*R*)-**1**	0.90	0.12	1.33	9.78	0.974
(*R*,*R*)-**1**+(*R*)-Mandelic acid (2:3)	3.67	0.58	1.58	1.14	1.099
(*R*,*R*)-**1**+(*S*)-Mandelic acid (2:3)	3.78	0.66	1.75	0.89	1.028
(*S*,*S*)-**1**	0.78	0.10	1.28	11.54	0.959
(*S*,*S*)-**1**+(*S*)-Mandelic acid (2:3)	3.76	0.57	1.51	1.15	1.094
(*S*,*S*)-**1**+(*R*)-Mandelic acid (2:3)	3.86	0.64	1.66	0.93	1.029

Benesi–Hildebrand type equation,[17] $1/\Delta F=1/\Delta F_{max}+(1/KC)(1/\Delta F_{max})$, in which $\Delta F=F_x-F_0$ and $\Delta F_{max}=F_\infty-F_0$; F_0, F_x and F_∞ are the emission intensities of (*R*,*R*)-**1** in the absence of mandelic acid, at an intermediate mandelic acid concentration and at a concentration of complete interaction, respectively, and *C* is the mandelic acid concentration. The value of *K* (±15%) was evaluated as 7.2×10^2 M^{-1} for (*R*,*R*)-**1** with (*S*)-mandelic acid (Fig. 4). The corresponding value for the system (*R*,*R*)-**1** with (*R*)-mandelic acid is 1.8×10^2 M^{-1}. The greater stability of the former association is apparent from the evaluated parameters.

To confirm further the type of association, an NMR study on the interaction of the (*R*,*R*)-**1** with mandelic acid in C_6D_6 (containing 2% [D_3]acetonitrile) has been made. An upfield shift of the methine proton signal of (*S*)-mandelic acid is noted at δ 5.19 as a consequence of the sensor interaction which shifts to δ 4.99 ($\Delta\delta$=0.20 ppm) for a 9:1 sensor/acid solution. The NMR shift values were utilized to frame a Job's plot analysis (Fig. 5), which corresponds to the formation of a complex in 2:3 ratio (sensor/acid, Scheme 2).[18] Experiments carried out under identical conditions with the chirality-matched mixture of (*R*,*R*)-**1** and (*R*)-mandelic acid lead to a small shift for the methine proton of the (*R*)-mandelic acid. This suggests that in the sensor–mandelic acid complex, (*S*)-mandelic acid is probably located much deeper inside the cavity of (*R*,*R*)-**1** than (*R*)-mandelic acid which significantly shields the methine proton of

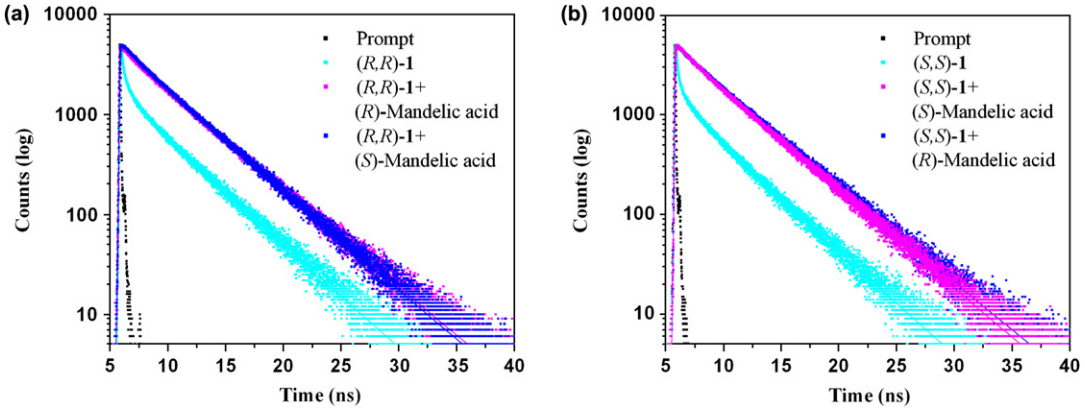

Figure 3. Time-resolved fluorescence decay of (a) (*R*,*R*)-**1** and its complexes with (*S*)-mandelic acid and (*R*)-mandelic acid (2:3 sensor/acid ratio) and (b) (*S*,*S*)-**1** and its complexes with (*R*)-mandelic and (*S*)-mandelic acids (2:3 sensor/acid ratio) in benzene containing 2% DME (λ_{ex}=440 nm). The sharp profile on the left is the lamp profile.

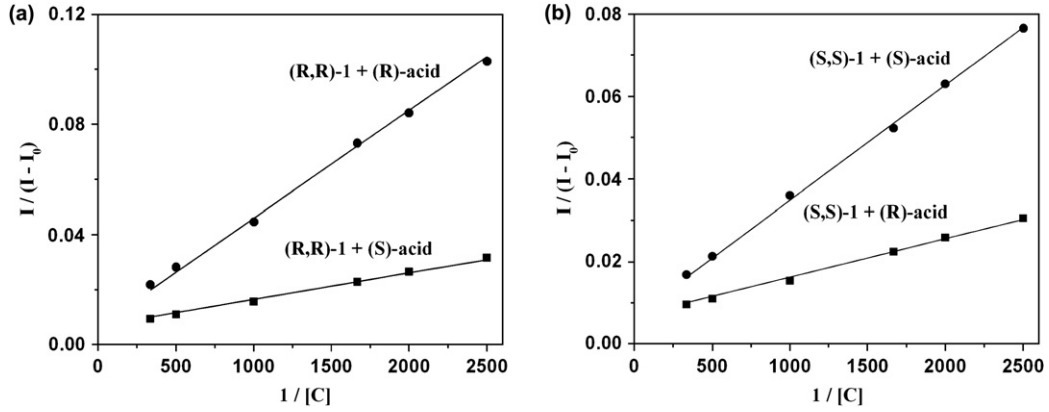

Figure 4. Benesi–Hildebrand plot of (a) (*R*,*R*)-**1** and (b) (*S*,*S*)-**1** (1.0×10^{-4} M in benzene containing 2% DME) in the presence of mandelic acid (I_0: fluorescence intensity of the sensor in the absence of the acid, *I*: fluorescence intensity of the sensor in the presence of the acid).

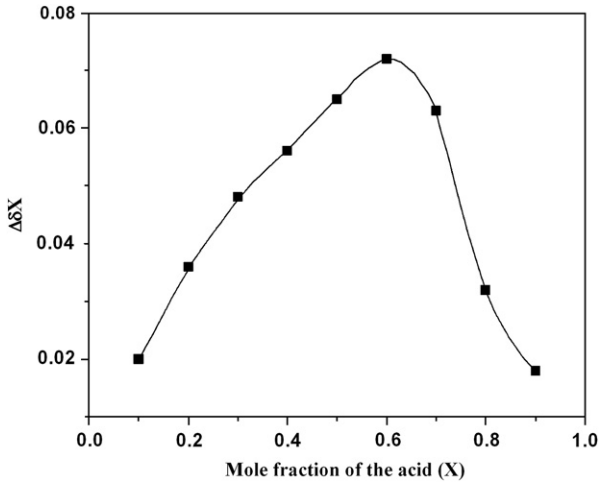

Figure 5. Job plot of (*R*,*R*)-**1** with (*S*)-mandelic acid at a constant concentration of 2.0×10^{-3} M in C_6D_6 containing 2% [D_3]acetonitrile measured by ^{1}H NMR spectra. The mole fraction of the acid, X, is plotted against $\Delta\delta$X. $\Delta\delta$ is the chemical shift change of the methine proton of the acid.

(*S*)-mandelic acid by the aromatic rings. This could be the origin of the dramatic difference in the fluorescence response of (*R*,*R*)-**1** towards the two enantiomers of mandelic acid.

Both (*R*)- and (*S*)-**2** were found to enhance the fluorescence of (*R*,*R*)-**1** under identical conditions that were used in the study with mandelic acid. Note here that the fluorescence enhancement does not indicate any enantioselectivity. Compound **3** was also introduced to interact with the sensor (*R*,*R*)-**1**. In the presence of racemic **3**, no fluorescence enhancement was detected. It is quite logical to infer from these experiments that the characteristic enantioselective fluorescence enhancement exhibited by the sensor molecule owes its origin to both the −OH and −COOH groups of mandelic acid. The proposed structure of the complex between (*R*,*R*)-**1** and (*S*)-mandelic acid formed through a multiple bonding process can be framed and shown in Scheme 2.

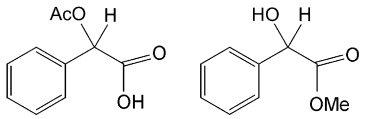

Further FTIR spectroscopic investigation (Fig. 6) of (*R*,*R*)-**1**+(*S*)-mandelic complex reveals that >C=N and >C=O peaks have shifted from 1633 to 1572 cm^{-1} and 1725 to 1617 cm^{-1}, respectively, indicating the formation of hydrogen bonds through acid group of mandelic acid and imine group of the

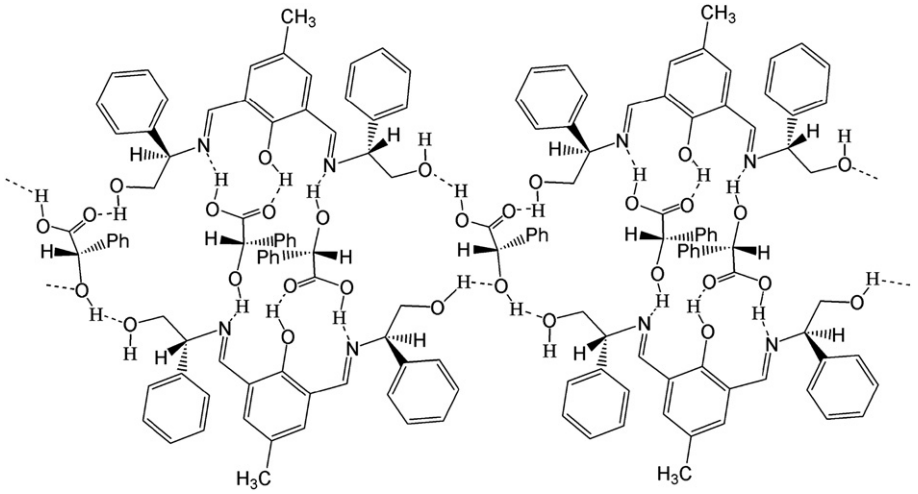

Scheme 2. Proposed structure for (*R*,*R*)-**1**+(*S*)-mandelic acid.

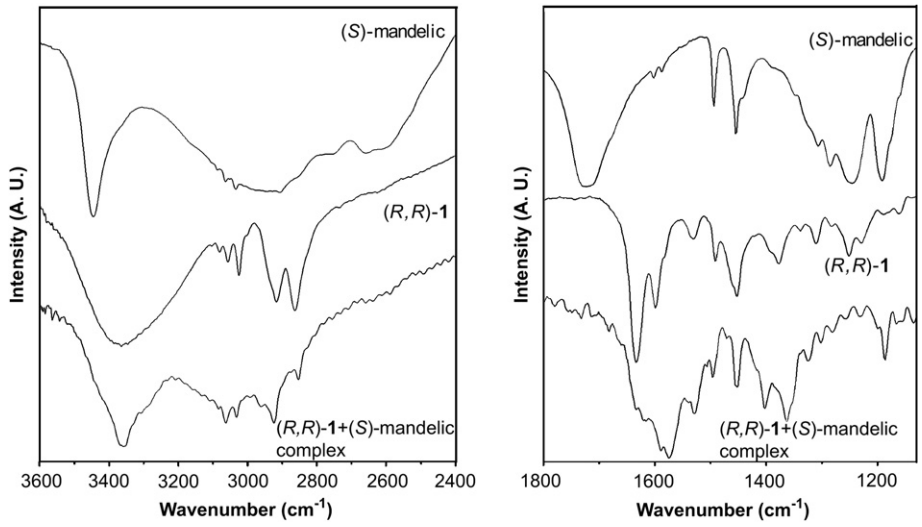

Figure 6. FTIR spectra of (*S*)-mandelic acid, (*R*,*R*)-**1** and (*R*,*R*)-**1**+(*S*)-mandelic acid complex (2:3 sensor/acid ratio).

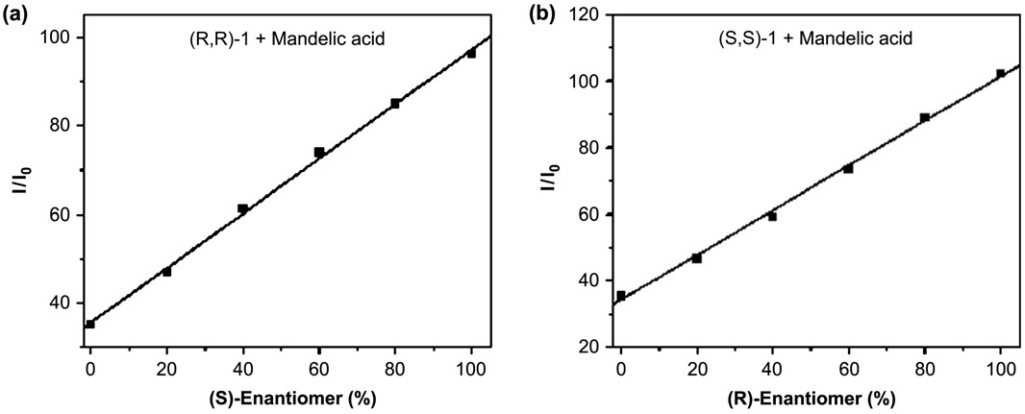

Figure 7. Fluorescence enhancement of (a) (*R*,*R*)-**1** and (b) (*S*,*S*)-**1** (1.0×10^{-4} M in benzene containing 2% DME) versus the enantiomeric composition of mandelic acid (3.0×10^{-3} M).

sensor. A comparison of the 3100–3600 cm^{-1} region shows that the alcoholic –OH group of acid and phenolic –OH group of sensor have also shifted from 3448 to 3362 cm^{-1} and 3380 to 3362 cm^{-1}, respectively. The results clearly indicate that the sensing properties of **1** are due to variant H-bonding interactions.

The fluorescence enhancement (I/I_0) of (*R*,*R*)-**1** as a function of the concentration of (*S*)- and (*R*)-mandelic acid is plotted (Fig. 7). As the concentration of the acid increases, the (*S*) enantiomer greatly enhances the fluorescence of (*R*,*R*)-**1**, but the (*R*) enantiomer does not. Similarly, the fluorescence enhancement of (*S*,*S*)-**1** significantly increases in presence of (*R*) enantiomer as the concentration of acid increases. We have further designed some experiments whereby the fluorescence intensity of (*S*,*S*)-**1** has been monitored in the presence of mandelic acid with various enantiomeric excesses. The results show a linear relationship between I/I_0 and the amount of *S*-component of mandelic acid. This would enable one to ascertain the enantiomeric ratio. The fluorescence of (*R*,*R*)-**1** in the presence of mandelic acid with various enantiomeric compositions has been studied which shows a linear relationship between I/I_0 and the percent of the *S*-component of mandelic acid enabling one to determine the enantiomeric composition.

3. Conclusion

We have been able to synthesize a chiral Schiff-base compound. It acts as a fluorescent sensor in ascertaining the enantiomeric composition of (*R*)- and (*S*)-mandelic acid and may find analytical applications over a definite concentration range. This type of sensor could be useful to facilitate transport or molecular mixture separations.

4. Experimental section

4.1. Materials and physical methods

All reagents and chiral substrates were purchased from Aldrich. All solvents were HPLC grade. FTIR spectra were obtained on a Nicolet MAGNA-IR 750 spectrometer with samples prepared as KBr pellets. Elemental analysis was carried out in a 2400 Series-II CHN analyzer, Perkin–Elmer,

USA. Luminescence spectra were performed using a Perkin–Elmer LS 55 Luminescence Spectrometer. Fluorescence lifetimes were determined from time-resolved intensity decay by the method of time-correlated single-photon counting using a picosecond diode laser at 440 nm as light source.

4.2. Synthesis and characterization of sensor (*R*,*R*)-**1**

4-Methyl-2,6-diformylphenol was synthesized starting from *p*-cresol following a published procedure.[19] To a solution of 4-methyl-2,6-diformylphenol (0.328 g, 2 mmol) in 25 mL of methanol was added (*R*)-2-amino-2-phenylethanol (0.549 g, 4 mmol) in 10 mL acetonitrile. The reaction mixture was refluxed for 2 h. The solution was filtered and kept overnight at 4 °C for few days. Yellow crystalline compound, (*R*,*R*)-**1**, was obtained in a good yield. Yield=0.76 g, 94%. Mp 67–69 °C. Anal. Calcd for $C_{25}H_{26}N_2O_3$: C, 74.60; H, 6.51; N, 6.96. Found: C, 74.23; H, 6.45; N, 6.89%; FTIR (KBr phase) (ν/cm^{-1}): 1635, 1600; ^{1}H NMR (300 MHz, $CDCl_3$) δ: 2.30 (s, 3H, Ar–CH_3), 3.89–3.99 (m, 4H, CH_2), 4.49 (t, J=6.3 Hz, 2H, CH), 7.26–7.46 (m, 12H, Ar–H), 8.63 (s, 2H, HC=N); ^{13}C NMR (75 MHz, $CDCl_3$) δ: 20.4 (CH_3), 67.7 (CH_2), 76.2 (CH), 127.3 (CH), 127.8 (CH), 128.8 (CH), 132.3 (C), 133.5 (CH), 138.5 (C), 140.0 (C), 159.5 (C), 166.3 (CH); $[\alpha]_D^{25}$ +74 (*c* 1.36, CH_3OH).

4.3. Synthesis and characterization of sensor (*S*,*S*)-**1**

Compound (*S*,*S*)-**1** was synthesized similarly starting from (*S*)-2-amino-2-phenylehanol and the same diformylphenol. Yield=0.74 g, 92%. Mp 67–70 °C. Anal. Calcd for $C_{25}H_{26}N_2O_3$: C, 74.60; H, 6.51; N, 6.96. Found: C, 74.23; H, 6.45; N, 6.89%; FTIR (KBr phase) (ν/cm^{-1}): 1635, 1600; ^{1}H NMR (300 MHz, $CDCl_3$) δ: 2.29 (s, 3H, Ar–CH_3), 3.88–3.98 (m, 4H, CH_2), 4.48 (t, J=6.3 Hz, 2H, CH), 7.22–7.44 (m, 12H, Ar–H), 8.60 (s, 2H, HC=N); ^{13}C NMR (75 MHz, $CDCl_3$) δ: 20.5 (CH_3), 67.6 (CH_2), 76.2 (CH), 127.3 (CH), 127.7 (CH), 128.7 (CH), 132.4 (C), 133.4 (CH), 138.5 (C), 140.0 (C), 159.5 (C), 166.3 (CH); $[\alpha]_D^{25}$ −76 (*c* 1.60, CH_3OH).

4.4. Preparation of samples for fluorescence measurement

Benzene stock solution of (*R*,*R*)-**1** and (*S*,*S*)-**1** was freshly prepared for each measurement. Chiral α-hydroxycarboxylic acids were freshly prepared containing 2% (v/v) DME (DME was added to improve the solubility of the acid in benzene). The solution of (*R*,*R*)-**1** and (*S*,*S*)-**1** was mixed with chiral acid solution at room temperature and resulting solutions were allowed to stand at room temperature for 3 h before fluorescence measurement.

4.5. Fluorometric analysis

Emission quantum yields (Φ) were estimated by integrating the area under the fluorescence curves using the formula:

$$\Phi_{\text{sample}} = \frac{\text{OD}_{\text{standard}} \times A_{\text{sample}}}{\text{OD}_{\text{sample}} \times A_{\text{standard}}} \times \Phi_{\text{standard}}$$

where A is the area under the emission spectral curve and OD is optical density of the compound at the excitation wavelength.[20] The standard used for the fluorescence quantum yield measurement is $[Ru(bpy)_3]Cl_2$ (Φ=0.042 in water) (λ_{ex}=450 nm).[21]

Acknowledgements

K.D., K.S. and M.N. acknowledge the Council of Scientific and Industrial Research and DST, New Delhi for financial support.

References and notes

1. (a) Wang, Q.; Chen, X.; Tao, L.; Wang, L.; Xiao, D.; Yu, X.-Q.; Pu, L. *J. Org. Chem.* **2007**, *72*, 97–101; (b) Heo, J.; Mirkin, C. A. *Angew. Chem., Int. Ed.* **2006**, *45*, 941–944; (c) Lin, Z.-B.; Lin, J.; Pu, L. *Angew. Chem., Int. Ed.* **2005**, *44*, 1690–1693; (d) Lin, Z.-B.; Pu, L. *J. Mater. Chem.* **2005**, *15*, 2860–2864; (e) Li, Z.-B.; Lin, J.; Qin, Y.-C.; Pu, L. *Org. Lett.* **2005**, *7*, 3441–3444; (f) Zhao, J.; Davidson, M. G.; Mahon, M. F.; Kociok-Kohn, G.; James, T. D. *J. Am. Chem. Soc.* **2004**, *126*, 16179–16186; (g) Lin, J.; Hu, Q.-S.; Xu, M.-H.; Pu, L. *J. Am. Chem. Soc.* **2002**, *124*, 2088–2089; (h) Lin, J.; Zhang, H.-C.; Pu, L. *Org. Lett.* **2002**, *4*, 3297–3300.
2. (a) Beer, G.; Rurack, K.; Daub, J. *Chem. Commun.* **2001**, 1138–1139; (b) Meskers, S. C. J.; Dekkers, H. P. J. M. *J. Am. Chem. Soc.* **1998**, *120*, 6413–6414; (c) Parker, K. S.; Townshend, A.; Bale, S. J. *Anal. Proc.* **1995**, *32*, 329–332; (d) James, T. D.; Sandanayake, K. R. A. S.; Shinkai, S. *Nature* **1995**, *374*, 345–347.
3. (a) Finn, M. G. *Chirality* **2002**, *14*, 534–540; (b) Reetz, M. T.; Becker, M. H.; Klein, H.-W.; Stöckigt, D. *Angew. Chem., Int. Ed.* **1999**, *38*, 1758–1761; (c) Reetz, M. T.; Zonta, A.; Schimossek, K.; Liebeton, K.; Jaeger, K.-E. *Angew. Chem., Int. Ed.* **1997**, *36*, 2830–2832; (d) Reetz, M. T.; Kuhling, K. M.; Deege, A.; Hinrichs, H.; Belder, D. *Angew. Chem., Int. Ed.* **2000**, *39*, 3891–3893.
4. Korbel, G. A.; Lalic, G.; Shair, M. D. *J. Am. Chem. Soc.* **2001**, *123*, 361–362.
5. (a) Copeland, G. T.; Miller, S. J. *J. Am. Chem. Soc.* **1999**, *121*, 4306–4307; (b) Stauffer, S. R.; Beare, N. A.; Stambuli, J. P.; Hartwig, J. F. *J. Am. Chem. Soc.* **2001**, *123*, 4641–4642; (c) Klein, G.; Reymond, J.-L. *Helv. Chim. Acta* **1999**, *82*, 400–407; (d) A review on the combinatory chiral catalyst screening: Shimizu, K. D.; Snapper, M. L.; Hoveyda, A. H. *Chem.—Eur. J.* **1998**, *4*, 1885–1889.
6. (a) Guo, J.; Wu, J.; Siuzdak, G.; Finn, M. G. *Angew. Chem., Int. Ed.* **1999**, *38*, 1755–1758; (b) Reetz, M. T.; Becker, M. H.; Kuhling, K. M.; Holzwarth, A. *Angew. Chem., Int. Ed.* **1998**, *37*, 2647–2650; (c) Ding, K.; Ishii, A.; Mikami, K. *Angew. Chem., Int. Ed.* **1999**, *38*, 497–501; (d) Abato, P.; Seto, C. T. *J. Am. Chem. Soc.* **2001**, *123*, 9206–9207.
7. Reetz, M. T. *Angew. Chem., Int. Ed.* **2001**, *40*, 284–310.
8. (a) Pu, L. *Chem. Rev.* **1998**, *98*, 2405–2494; (b) Kocovsky, P.; Vyskocil, S.; Smrcina, M. *Chem. Rev.* **2003**, *103*, 3213–3245; (c) Chen, Y.; Yekta, S.; Yudin, A. K. *Chem. Rev.* **2003**, *103*, 3155–3212; (d) Brunel, J. M. *Chem. Rev.* **2005**, *105*, 857–898.
9. (a) Irie, M.; Yorozu, T.; Hayashi, K. *J. Am. Chem. Soc.* **1978**, *100*, 2236–2237; (b) Yorozu, T.; Hayashi, K.; Irie, M. *J. Am. Chem. Soc.* **1981**, *103*, 5480–5484; (c) Avnir, D.; Wellner, E.; Ottolenghi, M. *J. Am. Chem. Soc.* **1989**, *111*, 2001–2003; (d) Iwanek, W.; Mattay, J. *J. Photochem. Photobiol., A: Chem.* **1992**, *67*, 209–226; (e) James, T. D.; Sandanayake, K. R. A. S.; Iguchi, R.; Shinkai, S. *J. Am. Chem. Soc.* **1995**, *117*, 8982–8987; (f) Kubo, Y. *Synlett* **1999**, 161–174.

10. (a) Pu, L. *Chem. Rev*. **2004**, *104*, 1687–1716; (b) Pugh, V.; Hu, Q.-S.; Pu, L. *Angew. Chem., Int. Ed.* **2000**, *39*, 3638–3641; (c) Xu, M.-H.; Lin, J.; Hu, Q.-S.; Pu, L. *J. Am. Chem. Soc*. **2002**, *124*, 14239–14246.
11. (a) Mei, X.; Wolf, C. *J. Am. Chem. Soc*. **2004**, *126*, 14736–14737; (b) Reetz, M. T.; Sostmann, S. *Tetrahedron* **2001**, *57*, 2515–2520; (c) Xu, Y. F.; McCarroll, M. E. *J. Phys. Chem. A* **2004**, *108*, 6929–6932.
12. Roy, P.; Dhara, K.; Manassero, M.; Ratha, J.; Banerjee, P. *Inorg. Chem*. **2007**, *46*, 6405–6412.
13. Coppola, G. M.; Schuster, H. F. *α-Hydroxyl Acids in Enantioselective Synthesis*; VCH: Weinheim, Germany, 1997.
14. (a) Hanessian, S. *Total Synthesis of Natural Products: The Chiron Approach*; Pergamon: Oxford, UK, 1983; (b) Taran, F.; Gauchet, C.; Mohar, B.; Meunier, S.; Valleix, A.; Renard, P. Y.; Gréminon, C.; Grassi, J.; Wagner, A.; Mioskowski, C. *Angew. Chem., Int. Ed.* **2002**, *41*, 124–127.
15. *Photoinduced Electron Transfer. Parts A–D*; Fox, M. A., Chanon, M., Eds.; Elsevier: Amsterdam, The Netherlands, 1988.
16. Turro, N. J. *Modern Molecular Photochemistry*; Benjamin/Cummings: Menlo Park, CA, 1978.
17. (a) Benesi, H. A.; Hildebrand, J. H. *J. Am. Chem. Soc*. **1949**, *71*, 2703–2707; (b) Fery-Forgues, S.; Le Bris, M.-T.; Guette, J.-P.; Valeur, B. *J. Phys. Chem.* **1988**, *92*, 6233–6237.
18. Connors, K. A. *Binding Constants: The Measurement of Molecular Complex Stability*; Wiley-Interscience: New York, NY, 1987; pp 24–28.
19. Gagne, R. R.; Spiro, C. L.; Smith, T. J.; Hamann, C. A.; Thies, W. R.; Schiemke, A. K. *J. Am. Chem. Soc*. **1981**, *103*, 4073–4081.
20. Austin, E.; Gouterman, M. *Bioinorg. Chem.* **1978**, *9*, 281–298.
21. Houten, J. V.; Watts, R. *J. Am. Chem. Soc*. **1976**, *98*, 4853–4858.